Theor Appl Climatol (2009) 95:279–289
DOI 10.1007/s00704-008-0006-8

ORIGINAL PAPER

Evaluation of urban thermal environments in commercial and residential spaces in Okayama City, Japan, using the wet-bulb globe temperature index

Y. Ohashi · T. Kawabe · Y. Shigeta · Y. Hirano · H. Kusaka · H. Fudeyasu · K. Fukao

Received: 5 February 2007 / Accepted: 30 December 2007 / Published online: 24 April 2008

Abstract We estimated wet-bulb globe temperature (WBGT) using measured meteorological data to understand the bioclimates of human living spaces during the summer season. Our research focused on commercial and residential areas of Okayama City, Japan (population ~700,000). The commercial spaces (CO) mainly consisted of multi-story office buildings, whereas the residential spaces (RE) consisted of one- or two-story residential buildings. On a fine day with southeast winds, the spatially averaged WBGT measured in the CO was higher than that in the RE. The difference was statistically significant and would have caused noticeable discomfort and a high risk of heat disorder for occupants of the CO over the long term. For instance, at 1900 Japan Standard Time (JST), the maximum difference in the WBGT between the CO and RE sites was 2.0°C (23.5°C for the CO and 21.5°C for the RE). From 1800 to 1900 JST, the wet-bulb temperature in the CO was still 1.5–2.0°C higher than that in the RE, even though both areas had the same dry-bulb temperature. This indicates that the CO retained greater amounts of water vapor for longer periods compared to the RE. The wet-bulb temperature in the CO increased rapidly at most observation points when the southeast sea breeze arrived. In contrast, in the RE, the wet-bulb temperature decreased until evening. This difference was caused by moist air transported from a river about 1 km upwind from the CO. The moist air forced an increase in the WBGT and elevated the risk of heat disorder in the CO. The spatially averaged globe temperature of the CO at 1500 JST was 6.2°C lower than that at the RE, causing the WBGT of the CO to decrease. The results suggest that the higher WBGT in the CO was caused by higher wet-bulb temperatures. On a day with southwest winds, the CO and RE showed no difference in WBGT because the river was not included in the upwind source area.

Y. Ohashi (✉) · T. Kawabe · Y. Shigeta
Faculty of Informatics, Okayama University of Science,
Okayama, Japan
e-mail: ohashi@big.ous.ac.jp

Y. Hirano
Faculty of Engineering, Gunma University,
Kinyu, Japan

H. Kusaka
Center for Computational Sciences, University of Tsukuba,
Tsukuba, Japan

H. Fudeyasu
International Pacific Research Center,
University of Hawaii at Manoa,
Honolulu, Hawaii, USA

K. Fukao
Faculty of Engineering, Gifu University,
Gifu, Japan

1 Introduction

Heat indices, such as the temperature-humidity index and effective temperature, have been used to evaluate the climatic comfort of urban parks (Barradas 1991; Saaroni and Ziv 2003), livestock stress (de la Casa and Ravelo 2003; Somparn et al. 2004), and heat stress during outdoor activities (Hoshi and Inaba 2005). In Japan, the urban heat island phenomenon, caused by artificial land surfaces and anthropogenic heat release, has become a serious social problem, contributing to numerous incidents of heat disorder among urban residents in the summer season. In urban areas, it is thus important to minimize heat disorders by predicting local climate with heat indices. However, while heat indices are useful for predicting and avoiding the risk of heat disorder, the aforementioned heat indices

exclude the effect of solar radiation, which is a key factor in urban climate. To overcome this issue, the wet-bulb globe temperature (WBGT) includes temperature, humidity, and radiation effects, and is a popular index for predicting heat disorders in urban environments. This index was initially developed to control heat casualties during military training (Yaglou and Minard 1957) but has since been widely used, including in regard to sports and physical labor (e.g., Hughson et al. 1983; Smolander et al. 1991; Hoshi and Inaba 2005). Two factors contribute to the widespread use of the WBGT index: the International Organization of Standardization recommended it as a standard in 1989 (ISO 7243), and the index allows for easy estimation of the risk of heat disorder without solving heat balance equations for the human body.

To examine living-space climate in a mid-sized city, we investigated the urban climate of Okayama City (population ~700,000), Japan. The WBGT index was calculated from meteorological observations by the authors and their colleagues in commercial and residential spaces.

2 Meteorological observations

We conducted meteorological observations from 1000 to 2000 JST on September 3 (first observation), 2004, and from 0800 to 2000 JST on August 9 (second observation), August 30 (third observation), and September 17 (fourth observation), 2005, in urban commercial space consisting of multi-story office buildings and substantial human activities, and in suburban residential space consisting of one- and two-story housing in Okayama City (Fig. 1). In each type of space, we measured surface meteorological elements at a height of 1.5 m at eight (2004 observation) or nine points (2005 observations). The observation points in the commercial space extended over a 500-m square area, while those in the residential space extended over an 800-m square area. The observation points were chosen so as to include north-south streets, east-west streets, and street crossings (Fig. 2); we traveled by bicycle to the sites and measured meteorological elements at each site once an hour. We also estimated the sky-view factor at each observation site and photographed the sky with a fish-eye lens. While the commercial space had mean sky-view factors of 0.57 (first observation) and 0.44 (second, third, fourth observations), the residential space had values of 0.77 and 0.70 (Table 1). Hereafter, we refer to commercial and residential spaces as CO and RE, respectively. The observed spaces were located approximately 16 km from the south coast of the Seto Inland Sea, with the RE located about 2.5 km southwest of the CO.

The Okayama Meteorological Observatory is located near the CO (the solid circle in Fig. 2a). Figure 3 shows the sunshine duration (at a height of 70.8m; i.e., above the urban canopy layer) measured by the Okayama Meteorological Observatory during the observation periods. Sunshine duration at an hour represents the value over the previous hour; for example, the sunshine duration at 1500 JST indicates the value for 1400–1500 JST. A Pacific high pressure system covered Japan during the first and second observation periods, creating clear, calm conditions at Okayama City, as shown in Fig. 3. However, at 1800 JST during the second observation, our observation was interrupted by a short rain shower. Cloudy conditions occurred

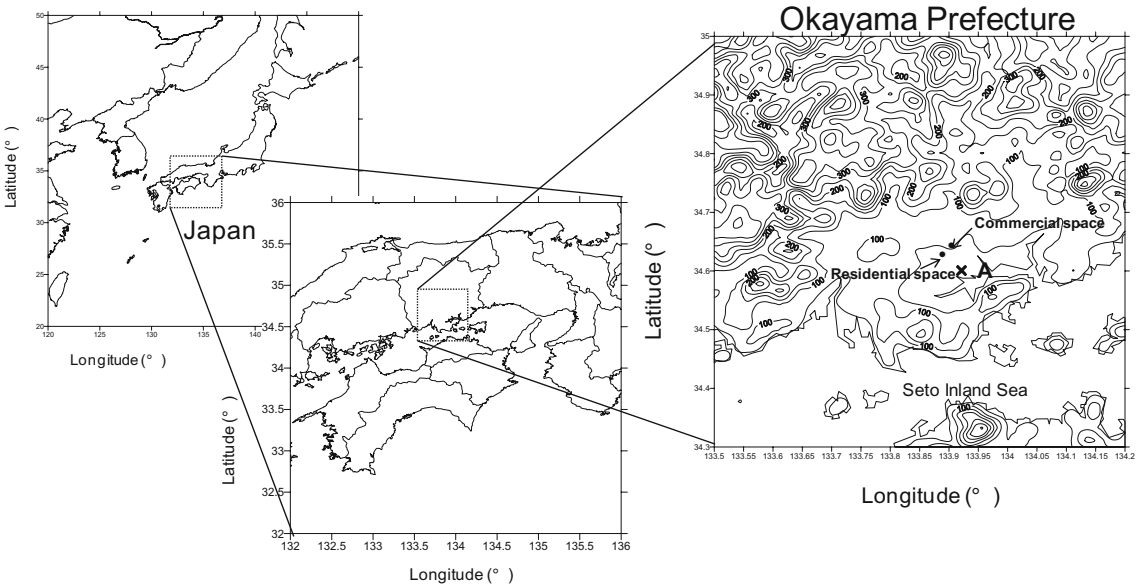

Fig. 1 Map showing the locations of the observation points in Okayama City, Japan

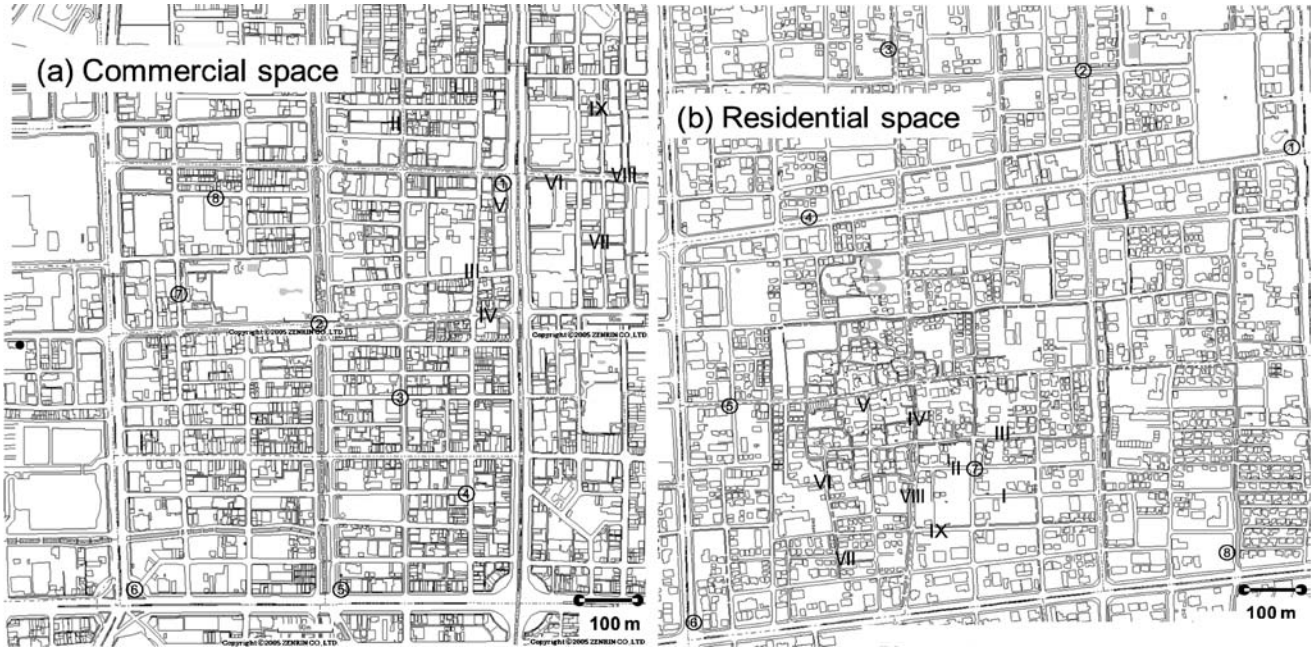

Fig. 2 Map of the observation points in (**a**) commercial (CO) and (**b**) residential (RE) spaces. Arabic numerals indicate the observation points in 2004, while Roman numerals represent the observation points in 2005. The *solid circle* in (**a**) shows the location of the Okayama Meteorological Observatory

during the third and fourth observations, with the third observation discontinued after 1400 JST because of rain.

We moved to the observation points by bicycle and measured the wind speed and direction, dry- and wet-bulb temperatures, and road-surface temperature at each point. We also checked whether the observation point was sunny or shaded. Table 2 summarizes the measured meteorological elements. The dry- and wet-bulb temperatures and the road-surface temperature were measured by a thermistor thermometer. Wind speed and direction were recorded as the mean speed and the most frequent direction within a 3-min period, respectively. The meteorological elements were recorded every 15 s; the data were then analyzed as time-mean values for 3 min.

3 Results

The WBGT under outdoor conditions is given by the following formula:

$$WBGT = 0.7T_w + 0.2T_g + 0.1T_d. \quad (1)$$

Here, T_w (°C) is the wet-bulb temperature, T_g (°C) is the globe temperature, and T_d (°C) is the dry-bulb temperature. Normally, T_d and T_w are measured under natural ventilation, with the T_w thermometer exposed to solar radiation and the T_d thermometer shaded from radiation. To obtain standard, accurate temperatures, we measured T_d and T_w under forced ventilation and placed the instrument sensors in a radiation shield. We then converted the measured temperatures into natural values as follows:

$$T_d = T_{dv} + 0.1326T_g - 3.7442 \quad (2)$$

and

$$T_w = T_{wv} + 0.0423T_g - 0.6703, \quad (3)$$

where T_{dv} and T_{wv} are the forcibly ventilated and shaded temperatures from our observations, respectively. Equations (2) and (3) were obtained from regression analysis in our previous research. Here, T_g in Eqs (2) and (3) were measured by using the Belnon-type globe temperature.

Normally, T_g is measured with a globe thermometer. However, the direct measurement of T_g is difficult for

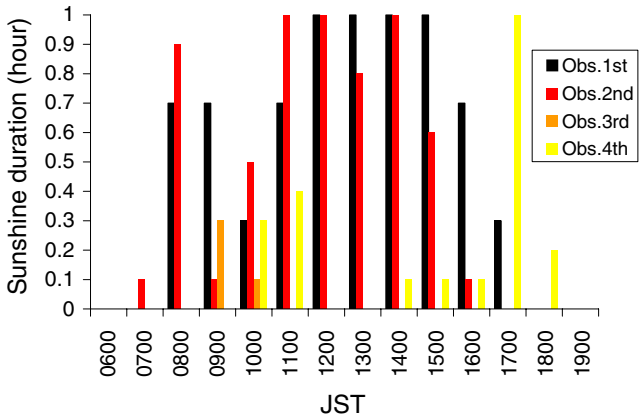

Fig. 3 Sunshine duration measured at the roof level (70.8 m) of the Okayama Meteorological Observatory

Table 1 Characteristics of the sky-view factor in the CO and the RE

	1st Obs.		2nd/3rd/4th Obs.	
	CO	RE	CO	RE
Average	0.57	0.77	0.44	0.70
S. D.	0.12	0.08	0.15	0.08
Maximum	0.76	0.84	0.67	0.76
Minimum	0.41	0.60	0.24	0.51

moving observations because of the need for long-term measurement. Accordingly, we used the estimation scheme for T_g proposed by Tonouchi et al. (2006):

$$T_g = T_{dv} + 0.017S - 0.208U, \tag{4}$$

where S (W m^{-2}) is the solar radiation, and U (m s^{-2}) is the wind speed. This scheme was constructed empirically from data including many actual observations and has been used for predicting heat disorder risk, as discussed on the website of the National Institute for Environmental Studies of Japan (http://www.nies.go.jp/health/HeatStroke/).

The surface wind speed measured at the observation points was used for U in Eq. (4). Since the calculation of globe temperature required estimation of the solar radiation, the hourly solar radiation (S_h) was calculated using the sunshine duration measured at a tower of the Okayama Meteorological Observatory:

$$S_h = S_{h,SD_h=0}(1 - SD_h) + S_{h,SD_h=1}SD_h, \tag{5}$$

$$S_{h,SD_h=0} = \left(0.1312 + 0.1762SD_{day}\right)S_0 + 0.00586, \tag{6}$$

and

$$S_{h,SD_h=1} = \left(0.7696 + 0.074SD_{day} - 0.00231T_{day}\right)S_0 - 0.2889, \tag{7}$$

where SD_h is the hourly sunshine duration (ranging from 0.0 to 1.0), S_0 is the hourly extraterrestrial horizontal radiation (J m^{-2} h^{-1}), SD_{day} is the ratio of the daily sunshine duration to the possible daily sunshine duration, and T_{day} is the daily average temperature (°C). $S_{h,SDh\,=\,0}$ and $S_{h,SDh\,=\,1}$ represent the hourly solar radiation under cloudy and clear-sky conditions, respectively. Thus, Eqs. (6) and (7) imply that the solar radiation amounts under cloudy and sunny conditions were averaged and weighted by the sunshine duration. These equations were proposed by Nimiya et al. (1997), who validated them based on data from numerous observation stations.

The solar radiation reaching a nearby road surface had to be estimated at each observation point. The S_h value of insolation in the horizontal plane was divided into solar radiation directed at and scattered onto the road:

$$S_h = S_{dir} + S_{sca}, \tag{8}$$

with the directed and scattered radiation used in Eq. (8) separated as follows (Japan Meteorological Agency 1999):

$$\frac{S_{sca}}{S_h} = a_0 + a_1K_T + a_2K_T^2 + a_3K_T^3 + a_4K_Th + a_5h + \Delta M. \tag{9}$$

In the above equation, K_T is the ratio of S_h to S_0, and h is the solar altitude (deg.). The constant values of a_0, a_1, a_2, a_3, a_4 and a_5 depend on the sunshine duration, and ΔM is the correction term for each month.

We also noted whether an observation point on the road was sunny or shaded. Accordingly, the solar radiation on the road, S, was calculated as follows:

$$S = S_{dir} + S_{sca}SVF, \quad \textit{if a sunny road}, \tag{10}$$

and

$$S = S_{sca}SVF, \quad \textit{if a shaded road}, \tag{11}$$

where SVF is the sky-view factor over the road at the observation point. The values of S obtained by Eqs. (10) and (11) were substituted into Eq. (4) to calculate the globe temperature.

Unfortunately, during the second observation, insolation conditions were not noted at the observation points. As shown in Fig. 3, the day of the second observation had clear weather similar to that for the first observation. The insolation conditions cannot be inferred from the results

Table 2 The meteorological elements measured in this study

	1st Obs. 2004 September 3	2nd Obs. 2005 August 9	3rd Obs. 2005 August 30	4th Obs. 2005 September 17
Dry-bulb temperature	○	○	○	○
Wet-bulb temperature	○	○	○	○
Road-surface temperature	○	×	×	○
Wind speed	○	○	○	○
Wind direction	○	○	○	○
Check of sunshine	○	×	○	○

of the first observation because the observation points differed. For this reason, we assumed that all observation points were sunny until 1600 JST at the CO and 1700 JST at the RE.

Figure 4 shows the WBGT values estimated for each CO and RE site using Eqs. (1) to (11). In the first observation, the CO and RE had the same spatially averaged WBGT in sunny areas until 1200 JST. Then, the WBGT in the RE gradually decreased until 1900 JST, whereas the WBGT in the CO did not decrease substantially after 1300 JST. The sunny WBGT in the CO was higher than that in the RE at 1500 JST and 1600 JST ($P<0.01$). On the other hand, the shaded WBGT at the CO was higher than that at the RE at 1700, 1800, and 1900 JST ($P<0.01$; two-sided T-test). The mean WBGT for the CO was 1.4°C higher than that for the RE at 1900 JST. At this time, the greatest difference in the WBGT estimated at each observation point was 2.0°C (23.5°C and 21.5°C for the CO and RE, respectively). Table 3 displays the WBGT value at each observation point of the CO and RE during the first observation period. The light, medium, and heavy shadings indicate "warning", "alert", and "severe alert" conditions, respectively, for outdoor activities (sports or daily life). "Safe" conditions exist below 21.0°C, "warning" conditions exist between 21.0 and 25.0°C, "alert" conditions exist between 25.0 and 28°C, "severe alert" conditions exist between 28.0 and 31.0°C, and "ban on sports" or "danger" conditions exist over 31.0°C. These ratings have been proposed by the Japan Sports Association (JASA) and the Japanese Society of Biometeorology (JSB). At all sunny points for both the CO and RE, "alert" conditions appeared until 1600 JST. All CO and RE points were shaded after 1700 JST, and "alert" conditions were changed back to "warning" conditions. However, the mean WBGT values of the CO began to exceed those of the RE after 1400 JST. This difference remained even when all observation points were shaded (1800–1900 JST).

In the second observation, the mean WBGT exceeded 27°C, corresponding to "alert" conditions. After 1000 JST, "severe alert" conditions appeared, followed by "ban on sports" or "danger" conditions beginning to appear around 1100 JST. There was little difference in the mean WBGT between the CO and RE during the second observation period (except for between 0900 and 1000 JST when data were missing for the CO). In the third observation, the mean WBGT was between 25 and 26°C until a rain shower

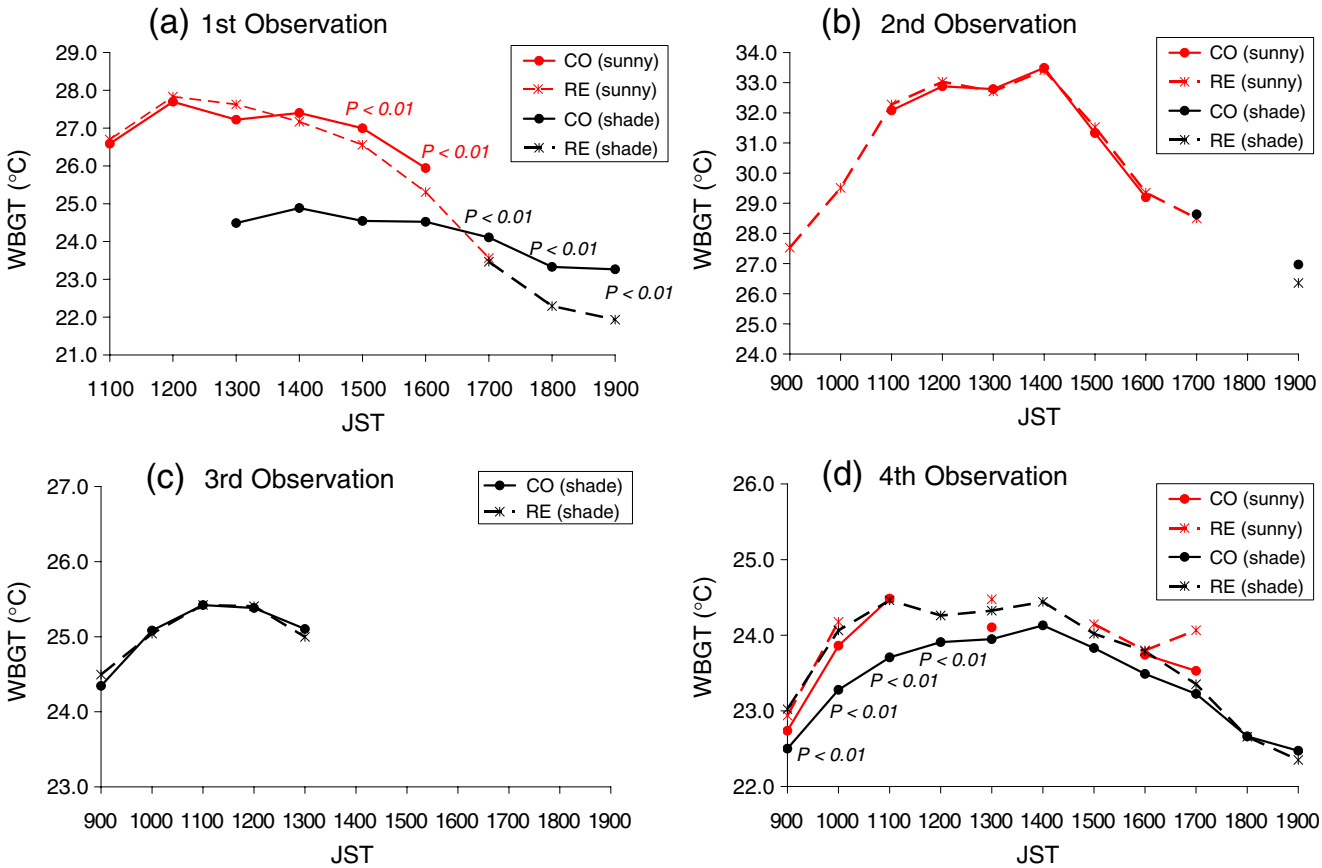

Fig. 4 Temporal variation of the spatially averaged WBGT estimated from observations at the CO and RE sites. The *solid* and *dashed lines* indicate the results for the CO and RE, respectively. The light and heavy lines represent sunny and shaded points, respectively

Table 3 WBGT calculated at each point in the (a) CO and (b) RE during first observation period

(a) Commercial space

	①	②	③	④	⑤	⑥	⑦	⑧	Sunny Ave.	Shade Ave.
1100JST	27.6	26.4	26.6	26.0	26.3	26.6	25.8	27.4	26.6	
1200JST	28.3	27.4	27.7	27.0	27.6	27.5	27.9	28.2	27.7	
1300JST	28.2	27.3	27.0	26.8	26.8	26.8	24.5	27.7	27.2	24.5
1400JST	25.6	27.6	27.6	27.2	27.6	27.0	24.2	27.3	27.4	24.9
1500JST	25.2	23.7	24.9	26.6	27.4	27.2	24.4	26.8	27.0	24.5
1600JST	24.4	24.1	25.0	25.5	26.3	26.1	24.8	24.3	25.9	24.5
1700JST	24.7	23.9	23.9	23.8	24.5	24.2	23.7	24.1		24.1
1800JST	23.3	23.5	23.6	23.7	23.5	23.1	22.5	23.1		23.3
1900JST	23.5	23.3	23.2	23.4	23.2	23.1	23.0	23.3		23.3

(b) Residential space

	①	②	③	④	⑤	⑥	⑦	⑧	Sunny Ave.	Shade Ave.
1100JST	26.0	27.0	26.3	26.7	26.7	27.2	27.2	26.6	26.7	
1200JST	27.2	28.2	27.9	28.0	28.3	27.4	27.9	27.7	27.8	
1300JST	27.6	28.2	27.2	27.8	28.2	27.9	26.6	27.5	27.6	
1400JST	27.3	27.6	26.2	26.6	27.1	27.6	×	27.7	27.2	
1500JST	26.4	26.6	26.1	26.3	26.7	27.0	26.7	26.6	26.6	
1600JST	24.8	26.0	25.0	25.3	24.9	25.4	25.5	25.6	25.3	
1700JST	22.7	23.9	23.2	23.8	23.9	23.9	23.0	23.3	23.6	23.5
1800JST	22.3	21.9	21.7	22.5	22.6	22.7	22.1	22.4		22.3
1900JST	22.0	21.5	21.5	22.0	22.0	22.7	21.7	21.9		21.9

Heavy, medium, light, and no shading indicate “severe alert”, “alert”, “warning”, and “safe” conditions for outdoor activities, respectively, based on guidelines from the Japan Sports Association and Japanese Society of Biometeorology

led to a discontinuance of observations. The mean WBGT values for the CO and RE were almost the same in the third observation. Because of cloudy conditions for the entire day, conditions fell between “warning” and “alert.” In the fourth observation, cloudy conditions produced some shade in both the CO and RE. Consequently, “warning” conditions occurred during the entire day. The mean WBGT in the RE was higher than that in the CO especially until 1200 JST ($P<0.01$).

Table 4 shows the spatially and temporally averaged values of all meteorological elements measured in the CO and RE. In the afternoon of the first observation, WBGT values in the CO were higher than those in the RE. The spatially averaged air temperatures in the CO, however, were 1°C lower than those in the RE between 1300 and 1600 JST. As shown in Fig. 5, the globe temperature calculated in the CO was lower than that in the RE. Therefore, the high WBGT in the CO was induced by the high specific humidity (water-vapor contents) in that space. Figure 5 also reveals that the wet-bulb temperature in the CO was 1°C higher than that in the RE after 1400 JST. In the second observation, the globe temperature differed little

Table 4 Mean values of the meteorological elements measured in the CO and the RE. Except for “hours of sun (shade),” the values in parentheses indicate the standard deviation of the mean

	Type of area	Mean air temperature (°C)	Mean road temperature (°C)	Mean specific humidity (g kg^{-1})	Mean wind speed (m s^{-1})	Mean wind direction	Hours of sunny (shade)
1st Obs.	CO	29.1 (0.6)	38.2 (3.2)	12.5 (0.7)	1.0 (0.8)	SE-S-SW LARGE	42 (46)
	RE	29.7 (0.7)	40.5 (2.2)	10.9 (0.3)	1.0 (0.4)	E-SE-S	58 (30)
2nd Obs. (Lack of data in 1800 JST and 1000–1100 JST in CO)	CO	33.8 (0.5)	No data	17.1 (0.2)	0.4 (0.5)	S-SW LARGE	No data
	RE	33.0 (0.6)	No data	17.6 (0.2)	0.3 (0.3)	S-SW	No data
3rd Obs. (Lack of data in 1400–1900 JST)	CO	27.8 (0.3)	No data	22.8 (0.1)	0.4 (0.2)	SE-S-SW	4 (41)
	RE	27.5 (0.2)	No data	22.5 (0.2)	0.3 (0.2)	Not specified	8 (37)
4th Obs.	CO	27.4 (0.3)	32.2 (2.3)	12.3 (0.1)	0.4 (0.2)	SE-S-SW LARGE	21 (87)
	RE	27.3 (0.3)	35.6 (1.2)	12.5 (0.1)	0.3 (0.4)	SE-S	24 (84)

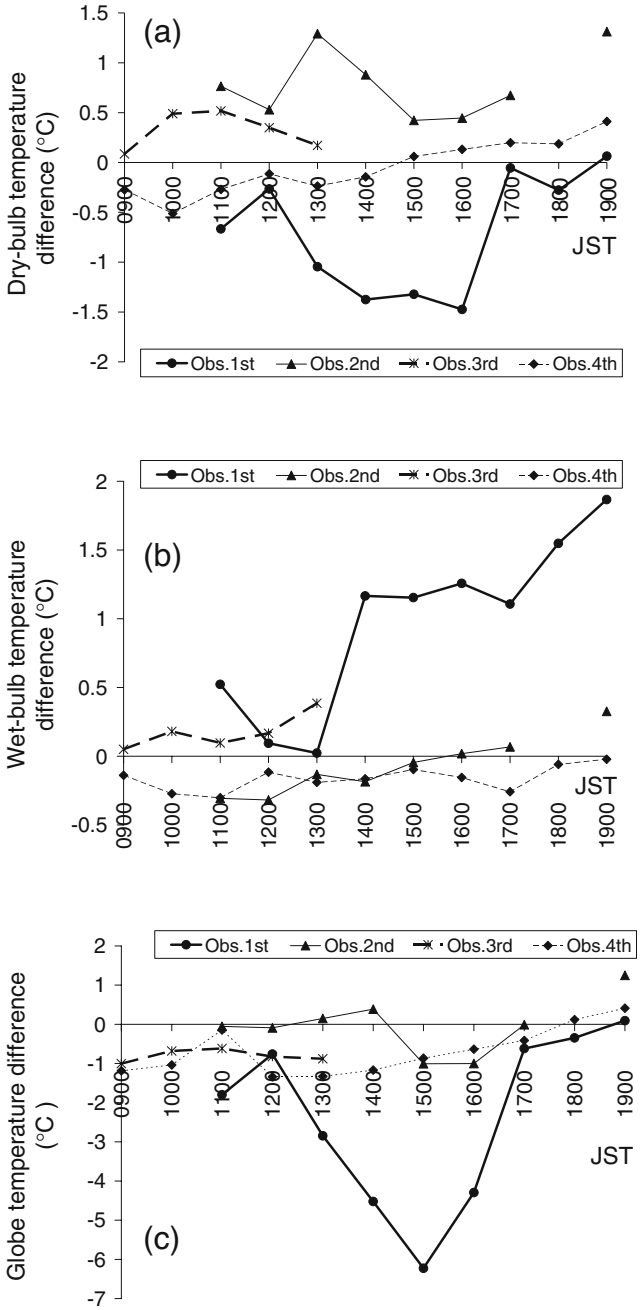

Fig. 5 Temporal variation of spatially averaged (**a**) dry-bulb temperature differences, (**b**) wet-bulb temperature differences, and (**c**) globe temperature differences between the CO and RE (CO minus RE)

between the CO and RE (Fig. 5c). Although the spatially and temporally averaged air temperature (dry-bulb temperature) in the CO was higher than that in the RE, the WBGT value in the CO was almost the same as that in the RE; the reason is that the specific humidity (wet-bulb temperature) in the CO was lower than that in the RE, as shown in Table 4 and Fig. 5.

During the third observation, both dry- and wet-bulb temperatures in the CO were higher than those in the RE. In contrast, the globe temperature calculated for the CO was lower than that for the RE, which resulted in the CO and RE having the same WBGT. In the fourth observation, all temperatures in the CO were lower than those in the RE during the morning. As a result, the spatially averaged WBGT in the CO was 0.8°C lower than that in the RE from 1000–1100 JST ($P<0.01$). In the following section, we discuss how the meteorological elements and the WBGT values differed between the CO and RE on each observation day.

4 Discussion

Figure 6 shows the relationship between the sky-view factor and the road surface temperature (Fig. 6a), WBGT (Fig. 6b), which are averaged for the observation period. The road temperature in the CO correlated positively with the sky-view factor. Also, the road temperatures in the CO were entirely lower than those in the RE. These mean the solar radiation insolates sufficiently onto the road surfaces in the RE. However, the WBGTs in the CO became to be almost higher than those in the RE. This result suggests that

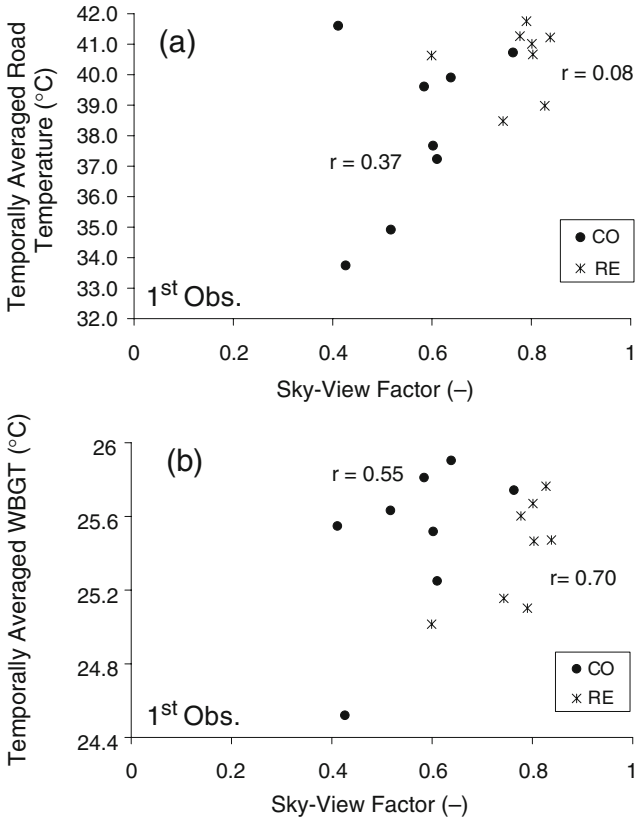

Fig. 6 Scatter diagrams of the sky-view factor and the (**a**) temporally averaged road surface temperature, (**b**) temporally averaged WBGT, in the first observation. The value of symbol *r* represents the correlation coefficient

Table 5 Parameter values used in Eqs. (12) and (13) for calculation of the source area (from Schmid 1994)

Parameters		Equation	α1	α2	α3	α4
a	Stable	(12)	0.773	1.24	0.957	1.25
	Unstable	(12)	0.853	1.23	0.441	1.00
e	Stable	(12)	30.4	1.23	2.60	0.452
	Unstable	(13)	40.4	1.22	15.5	−0.548
x_m	Stable	(12)	4.30	1.28	1.74	0.688
	Unstable	(13)	5.37	1.25	5.96	−0.472

the WBGT does not depend only on the radiation environment locally at the point. Within a day, meteorological fields are affected not only by the microscale environment but also by the upwind environment. Thus, we consider upwind areas that influenced the background meteorological fields of the observation points.

Schmid (1994) estimated the "source area" for passive scalars that influence observation data using a backward

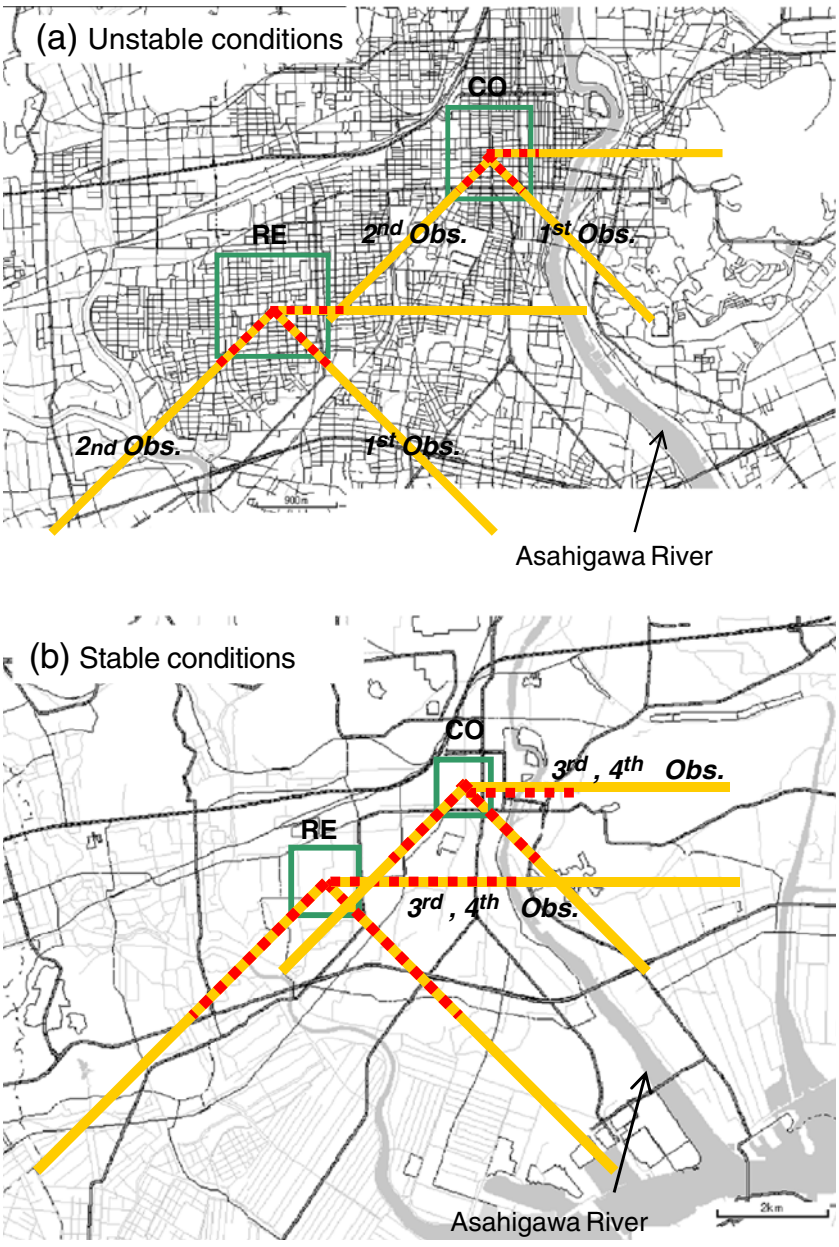

Fig. 7 Regions including the source area aligned from the upwind edge to the downwind edge for each site under (**a**) unstable and (**b**) stable conditions in the CO (z_0=1.0 m) and RE (z_0=0.2 m). *Solid lines* represent areas connecting the edges of the source-area length for z/L=0.1 in (**a**) and $-z/L$=4.0×10^{-4} in (**b**). *Dashed lines* represent those connecting the upward edges of source areas for z/L=2.0×10^{-4} in (**a**) and $-z/L$=1 in (**b**)

trajectory that considered the effects of turbulent diffusion. The parameters D_1 and D_2 of the source area vary with atmospheric stability:

$$D_1 = z_0\alpha_1\left(\frac{z}{z_0}\right)^{\alpha_2}\exp\left(\alpha_3\left(\frac{z}{L}\right)^{\alpha_4}\right) \quad (12)$$

and

$$D_2 = z_0\alpha_1\left(\frac{z}{z_0}\right)^{\alpha_2}\left(1-\alpha_3\frac{z}{L}\right)^{\alpha_4}, \quad (13)$$

where z_0 is the roughness length, and L is the Monin-Obukhov stability length. Table 5 lists the values of α_1, α_2, α_3, and α_4. Although z represents the actual observation height, we regarded this height as the sea-breeze height over the CO canopy layer (i.e., z=30m). In Eq. (12), D_1 corresponds to a (m) under stable and unstable conditions and to e (m) and x_m (m) under stable conditions, where a is the distance from the upwind edge of the source area to an observation point, e is the distance from the downwind edge of the source area to an observation point, and x_m is the maximum source location from an observation point. On the other hand, e and x_m under unstable conditions are calculated using Eq. (13) (i.e., D_2 is e and x_m). Here, we assume z_0 values of 1.0 and 0.2 m, respectively, for the CO and RE. The calculation results for the source area are summarized in Fig. 7 and Table 6.

The Pasquill stability classes (Pasquill 1961) when a sea breeze arrived at the CO and RE were estimated at location A (the Air Quality Monitoring System of Okayama Prefecture) shown in Fig. 1. The classes were determined by the shortwave radiation and wind speed measured at that time. When sea breezes covered location A, the Pasquill stability class was B or C, implying unstable or weak unstable conditions, respectively. This result reveals that unstable conditions still occur in the sea-breeze stage because of surface heating by solar radiation. That is, the first and second observations were under unstable conditions during the daytime. Consequently, a=35–56 (52–81) m, e=551–2553 (785–3637) m, and x_m=150–376 (226–563) m are valid for the CO (RE) from the calculations of Eqs. (12) and (13). In Fig. 7a, the values of e (i.e., the source area length parallel to the wind direction) were drawn according to the prominent wind direction of sea breezes, including the southeast and southwest sea breezes (data measured at the Okayama Meteorological Observatory) during the first and second observations, respectively. During the first observation, the source area of the CO included a nearby "Class A" great river (the Asahigawa River), while that of the RE included an area of many residential houses but not the river. Therefore, the southeast sea breeze tends to transport moist air supplied from the river into the CO, leading to higher wet-bulb temperatures in the CO than in the RE (Fig. 5b). As shown in Eq. (1), the wet-bulb temperature strongly affects the WBGT value (70%), whereas the dry-bulb temperature is not so important for the WBGT (10%). Thus, the WBGT in the CO exceeded that in the RE during the southern sea-breeze stage, despite the lower globe temperature of the CO.

In contrast, in the second observation, the higher dry-bulb temperature and slightly lower wet-bulb temperature measured in the CO probably resulted from the transport of warm, dry air from the many office buildings and heavy traffic within the upwind source area. However, these features had little effect on the WBGT difference between the CO and the RE.

The third and fourth observations were made under stable conditions created by clouds. Therefore, a=52–55

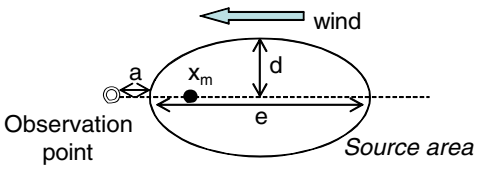

Table 6 Calculation results for the source-area parameters. The upper figure shows the locations of the source-area parameters

	CO		RE	
z/L	-1 ∼ -4×10^{-4} (unstable)	2×10^{-4}∼0.1 (stable)	-1 ∼ -4×10^{-4} (unstable)	2×10^{-4}∼0.1 (stable)
a (m)	36∼56	52∼55	52∼81	77∼81
x_m (m)	151∼377	336∼478	226∼563	527∼749
e (m)	551∼2,553	2,107∼4,995	785∼3,637	3,052∼7,233

(77–81) m, e=2107–4495 (3052–7233) m, and x_m=336–478 (527–749) m were estimated for the CO (RE) as shown in Table 6. During daytime, the east wind was prominent in both the third and fourth observations. In addition, under stable conditions, the source area extended further downwind compared with the source area for the unstable conditions in the first and second observations. As shown in Fig. 7b, the source areas in both the CO and RE included not only the river, but also quasi-homogeneous land-use surfaces (mainly rice paddies, fields, and forests). As a result, there was little difference in dry- and wet-bulb temperatures between the CO and RE.

5 Conclusions

We estimated the wet-bulb globe temperature (WBGT) using measured meteorological elements to understand the bioclimates of human living spaces during summer. Our research focused on commercial and residential spaces in Okayama City (population of ~700,000), Japan. The commercial spaces (CO) mainly consisted of multi-story office buildings, while the residential spaces (RE) consisted of one- or two-story residential buildings. The results are briefly summarized as follows.

– Under conditions of sunny days and southeast sea breezes:

The WBGT value in the CO was higher than that in the RE despite lower dry-bulb and globe temperatures in the CO; the difference appeared from 1300 JST only in sunny locations, and after 1700 JST in shaded locations. This relationship was caused by higher wet-bulb temperatures in the CO created by the sea-breeze transport of moist air originating from a river; because of the difference in upwind source areas, only the CO was affected by the moist river air, which was the main reason for the increased WBGT value and the enhanced the risk of heat disorders until evening in the CO.

– Under conditions of sunny days and southwest sea breezes:

The CO and RE had almost the same WBGT values. Although the dry-bulb temperature in the CO exceeded that in the RE, the wet-bulb temperature in the CO was lower than that in the RE because there were many buildings in the upwind source area. While warm air increased the WBGT, dry air decreased the WBGT in the CO. Consequently, WBGT values were similar in the CO and RE.

– Under conditions of cloudy days with east winds:

The WBGTs in the CO and RE were almost the same and similar to the results for sunny days with southwest sea breezes. This result is attributable to the similarity of the upwind sources areas for the CO and RE.

The above results demonstrate that the daily biometeorological environment in the study area is determined by not only radiation and microscale meteorological conditions but also by mesoscale flow conditions, as defined by the source area. Therefore, assessments of human discomfort within living spaces should include both the microscale biometeorological environment and overlying mesoscale meteorological conditions.

In the future, we will simulate the urban bioclimate characterized in this study using a mesoscale meteorological model coupled with an urban canopy model (e.g., Kusaka et al. 2001; Kondo et al. 2005; Ohashi et al. 2007).

Acknowledgements The meteorological data were provided by the Japan Meteorological Agency, Okayama Prefecture, and relevant cities.

References

Barradas VL (1991) Air temperature and humidity and human comfort index of some city parks of Mexico City. Int J Biometeorol 35:24–28

de la Casa AC, Ravelo AC (2003) Assessing temperature and humidity conditions for dairy cattle in Cordoba, Argentina. Int J Biometeorol 48:6–9

Hoshi A, Inaba Y (2005) Meteorological conditions and sports deaths at school in Japan, 1993–1998. Int J Biometeorol 49:224–231

Hughson RL, Staudt LA, Mackie JM (1983) Monitoring road racing in the heat. Phys Sportsmed 11:94–105

Japan Meteorological Agency (1999) Taiyoukou Hatsuden Shisutemu Jitsuyouka Gizyutsu Kaihatsu. New Energy and Industrial Technology Development Organization (NEDO) report (in Japanese)

Kondo H, Genchi Y, Kikegawa Y, Ohashi Y, Yoshikado H, Komiyama H (2005) Development of multi-layer urban canopy model for the analysis of energy consumption in a big city: structure of the urban canopy model and its basic performance. Boundary-Layer Meteorol 116:395–421

Kusaka H, Kondo H, Kikegawa Y, Kimura F (2001) A simple single-layer urban canopy model for atmospheric models: comparison with multi-layer and slab models. Boundary-Layer Meteorol 101:329–358

Nimiya H, Akasaka H, Matsuno Y, Soga K (1997) A method to estimate the hourly solar radiation using AMeDAS data. Part 2: Application to the improved sunshine recorder of AMeDAS (in Japanese). J Soc Heat Air-Cond Sanitar Eng Jpn 65:53–65

Ohashi Y, Genchi Y, Kikegawa Y, Kondo H, Yoshikado H, Hirano Y (2007) Influence of air-conditioning waste heat on air temperature in Tokyo office areas during summer: numerical experiments using an Urban Canopy Model coupled with a building energy model. J Appl Meteorol Climatol 46:66–81

Pasquill F (1961) The estimation of the dispersion of windborn material. Meteorol Mag 90:33–49

Saaroni H, Ziv B (2003) The impact of a small lake on heat stress in a Mediterranean urban park: the case of Tel Aviv, Israel. Int J Biometeorol 47:156–165

Schmid HP (1994) Source areas for scalars and scalar fluxes. Boundary-Layer Meteorol 67:293–318

Smolander J, Ilmarinen R, Korhonen O (1991) An evaluation of heat stress indices (ISO 7243, ISO/DIS 7933) in the prediction of heat strain in unacclimated men. Int Arch Occup Environ Health 63:39–41

Somparn P, Gibb MJ, Markvichitr K, Chaiyabutr N, Thummabood S, Vajrabukka C (2004) Analysis of climatic risk for cattle and buffalo production in northeast Thailand. Int J Biometeorol 49:59–64

Tonouchi M, Murayama K, Ono M (2006) WBGT forecast for prevention of heat stroke in Japan. Sixth Symposium on the Urban Environment, American Meteorological Society, session PJ1.1

Yaglou CP, Minard CD (1957) Control of casualties at military training centers. A.M.A Archives of Industrial Health 16:304–314